DOI: 10.1002/anie.201002685

Imaging in Microfluidics

Microfluidic Gas-Flow Imaging Utilizing Parahydrogen-Induced Polarization and Remote-Detection NMR**

Ville-Veikko Telkki, Vladimir V. Zhivonitko, Susanna Ahola, Kirill V. Kovtunov, Jukka Jokisaari, and Igor V. Koptyug*

Microfluidics is the science and technology of systems that process or manipulate small amounts of fluids using channels with dimensions of less than one millimeter.[1,2] Fluid transport in microfluidic devices is usually monitored by optical detection methods, such as laser-induced fluorescence.[3] Even though they are very useful in many cases, these methods set a limit to the manufacturing material of the chip under study, which must be optically transparent. Furthermore, optical methods generally require addition of markers, which can alter the hydrodynamic properties of the system.

Nuclear magnetic resonance (NMR) has several advantages compared with optical methods in microfluidic flow profiling, because it does not require the use of markers, it allows versatile experiments providing image, dynamic, and spectroscopic information, and radiofrequency (RF) waves can penetrate opaque materials.[4,5] However, conventional NMR measurements using a large coil around the microfluidic device are very challenging or even impossible because of low sensitivity resulting from the low filling factor of the coil (typically on the order of 10^{-5} to 10^{-4}) and the low sensitivity of large coils. The issue is even worse when gases, whose molecular number density is about three orders of magnitude lower than in liquid, are investigated.

Herein, we overcome the sensitivity issue for microfluidic gas flow by combining remote-detection (RD) magnetic resonance imaging (MRI)[6–10] and parahydrogen-induced polarization (PHIP)[11–14] techniques. In RD MRI, spatial information is encoded into fluid spins by magnetic field gradients and a large RF coil around the microfluidic device, corresponding to the phase encoding in a conventional MRI experiment. Thereafter, the spin coherences are stored as a longitudinal magnetization, and the amplitude of the magnetization is detected by an ultrasensitive solenoid microcoil outside the device.[9,10] As the fluid molecules flow from the encoding region to the detector, RD MRI provides time-of-flight (TOF) information, making it possible to obtain three-dimensional TOF images of fluid flow in the device.[8] In our setup (Figure 1b and Supporting Information), the encoding coil is a commercial imaging coil, and a small solenoid wound around the outlet capillary is used as a detection coil. The encoding coil $\pi/2$ pulse is about 600 times longer than that of the detection coil, implying that, according to the principle of reciprocity,[15] the sensitivity of the detection coil is 600 times better than that of the encoding coil.

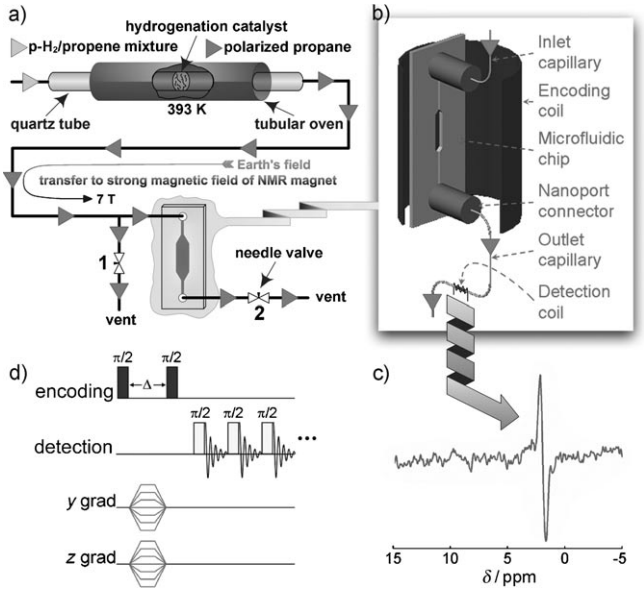

Figure 1. a) Experimental setup. The parahydrogen/propene mixture flows through the hydrogenation catalyst layer packed between plugs of glass wool inside a heated quartz tube. After the hydrogenation reaction, the polarized propane gas flows from the tube into the microfluidic chip inside an NMR magnet. b) Remote-detection MRI experimental setup. c) ^{1}H NMR spectrum of hyperpolarized propane gas measured by the detection coil. d) Remote-detection MRI pulse sequence, in which phase encoding of spatial coordinates is carried out in the *y* and *z* directions. Time-of-flight information is obtained by a train of $\pi/2$ pulses applied in the detection coil.

However, this rather large sensitivity improvement is not enough for microfluidic gas-flow MRI, and the additional sensitivity boost needed in the experiments was achieved by hyperpolarizing the probe fluid. To date, optical pumping of

[*] Dr. V.-V. Telkki, S. Ahola, Prof. J. Jokisaari
Department of Physics, NMR Research Group, University of Oulu
P.O. Box 3000, 90014 Oulu (Finland)
Fax: (+358) 8-553-1287
E-mail: ville-veikko.telkki@oulu.fi
Dr. V. V. Zhivonitko, Dr. K. V. Kovtunov, Prof. I. V. Koptyug
Magnetic Resonance Microimaging Group
International Tomography Center
3A Institutskaya St., Novosibirsk 630090 (Russia)

[**] This work was funded by the grants from the Academy of Finland (123847, 132132, and 116824), University of Oulu, RAS (5.1.1), RFBR (08-03-00661, 08-03-00539), SB RAS (67, 88), the program of support of leading scientific schools (NSh-7643.2010.3) and FASI (state contract 02.740.11.0262). I.V.K. thanks Prof. C. Bianchini and Dr. P. Barbaro (ICCOM-CNR, Sesto Fiorentino, Firenze, Italy) for providing the sample of catalyst [Rh(cod)(sulfos)]/SiO_2.

Supporting information for this article is available on the WWW under http://dx.doi.org/10.1002/anie.201002685.

noble gases is the polarization technique in gas-phase studies that is the most often used, and hyperpolarized xenon has already been utilized in combination with the RD MRI technique.[6–10,16–18] PHIP provides an alternative method for polarization enhancement in gas-phase MRI aside from the expensive hyperpolarized noble gases. This technique exploits the high-spin polarization derived from the para spin isomer of molecular hydrogen (H_2).[19,20] Originally, the polarization was achieved in a homogeneous hydrogenation reaction catalyzed by transition metal complexes. However, the fact that the catalyst is dissolved in the fluid restricts the use of a polarized product in many applications, although the catalyst can be removed from the solution in a favorable case.[21] Recently it was shown that a heterogeneous hydrogenation reaction can result in a gaseous, catalyst-free hyperpolarized product.[11–14] Herein, we utilize this PHIP technique along with the experimental scheme termed ALTADENA,[22] in which the hydrogenation step is performed outside an NMR instrument in the Earth's magnetic field and the reaction products are adiabatically transferred to the NMR magnet (Figure 1 a). The transfer has to be relatively fast, because the relaxation time of the polarized gas, propane in this case, is quite short (on the order of 900 ms). The polarization enhancement of propane provided by PHIP was measured to be about 80 as compared with thermal polarization in a 7 T magnetic field (Supporting Information). The estimated reaction yield (60 %) was higher than that obtained in previous experiments[12] (5 %), because of the different experimental implementations. Much better yield and slightly lower polarization enhancement altogether resulted in an about three times stronger signal obtained from the hyperpolarized propane herein.

First, we demonstrated that the overall sensitivity enhancement given by the microcoil and PHIP ($600 \times 80 = 48\,000$) is sufficient to observe a spectrum of continuously flowing polarized gas mixture (1 atm pressure) in the capillary. The gas volume inside the detection coil was only 53 nL. Strong ALTADENA signals were observed after 8 scans were accumulated (Figure 1 c). No signal from the thermally polarized nuclei is seen in the spectrum. In a stopped-flow experiment performed with the same gas mixture after the hyperpolarization had decayed, the thermally polarized gas produced comparable signals only after accumulating 4000 scans (Supporting Information). This kind of extensive accumulation would lead to the impossibly long RD MRI experiments, thus highlighting the indispensable role of PHIP. The signal-to-noise ratio (SNR) in the ALTADENA spectrum is about 25, corresponding to a theoretical SNR of 8.8 per scan and atmosphere. For comparison, the SNR of hyperpolarized xenon measured for the $Xe/He/N_2$ gas mixture in a continuous-flow experiment using an almost identical microcoil (the inside diameter was slightly larger) was 0.10 per scan and atmosphere,[9] meaning that the sensitivity in the hyperpolarized propane experiment was 88 times higher than in the hyperpolarized xenon experiment. This implies a 7700-fold reduction in the experimental time needed for a certain SNR. A theoretically estimated sensitivity ratio between the two experiments is smaller, namely about 11 (Supporting Information). In any case, we can conclude that the propane experiment is one to two orders of magnitude more sensitive than the xenon experiment.

In the second demonstration, the capillary tubing was set to lead through the encoding and detection coils, and, using the pulse sequence shown in Figure 1 d, two-dimensional RD TOF images of the flow of polarized propane gas through the encoding coil region were acquired (Figure 2 b and Supporting Information, Movie 1). By measuring the position of the maximum of the signal as a function of travel time, we estimated that the flow velocity inside the capillary was about 30 $cm\,s^{-1}$. The signal patches in the panels measured at different travel time instants are relatively short, showing that the dispersion of gas molecules is small. The Reynolds number of the gas mixture was estimated to be very small (about 0.7), indicating laminar flow. The flow would cause large dispersion if no diffusional mixing took place. Therefore, the images show that the transverse diffusional mixing is

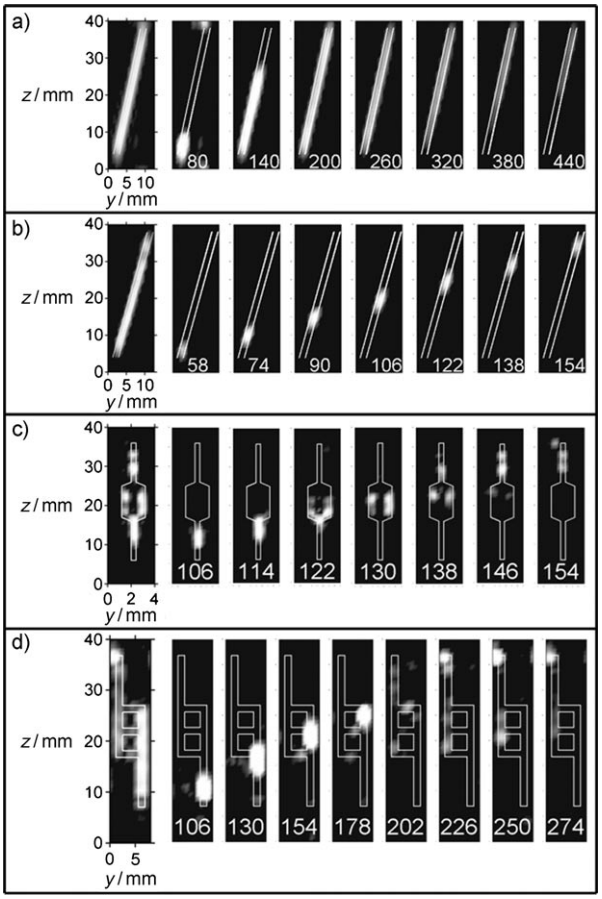

Figure 2. Remote-detection time-of-flight images measured from microfluidic systems. a) Water and b)–d) hyperpolarized propane flowing in the capillary tubing leading through the encoding coil (a,b) and microfluidic chips (Chip 1 (c) and Chip 2 (d)). The flow channels are outlined with white lines. The first images on the left are the result of summation of subsequent images measured at different travel-time instances (time projection). The travel time instances are indicated in milliseconds. The spatial resolution in the *y* and *z* directions is 0.5–1.6 mm and 1.5–2.5 mm, respectively, depending on the experiment.

efficient, which is reasonable as the average diffusion time of propane across the 150 μm capillary (about 1 ms) is much shorter than the travel time between encoding and detection coils (on the order of 100 ms), allowing complete mixing of different flow lamellas. For comparison, RD TOF images of water flowing through the capillary were also measured (Figure 2a and Supporting Information, Movie 2). This was possible to carry out without hyperpolarization, exploiting only the thermal polarization of water protons, because of high spin density in water. The resulting images show that the flow velocity in this experiment was smaller than in the gas experiment, namely about 17 cm s^{-1}. Another striking difference is that the dispersion is much larger; for example, at $t =$ 200 ms the signal from the whole encoding coil region is seen. This is a consequence of laminar flow (the Reynolds number is about 25) and the lack of diffusional mixing in water: The average diffusion time of water across the capillary (about 6 s) is now much longer than the travel time (on the order of 200 ms), thus preventing the mixing of flow lamellas.

In the third demonstration, propane gas flowed through Chip 1 containing an enlargement section between two narrow channel sections. The thickness of the channels was expected to be constant in different channel sections. The measured TOF images (Figure 2c and Supporting Information, Movie 3) revealed a surprising behavior of the fluid in the chip: the major gas flow streams passed close to the edges of the enlarged section, and almost no flow took place in the central part. One conceivable explanation is that for some reason the gas encoded in the central part does not arrive to detector before the NMR signal is destroyed by relaxation. Performed hydrodynamic simulations (Supporting Information) did not predict any flow behavior that could lead to this effect in the designed geometry. Instead, the images show that the manufactured geometry is not what was expected. The signal amplitude in the central part is almost zero (Figure 3a),

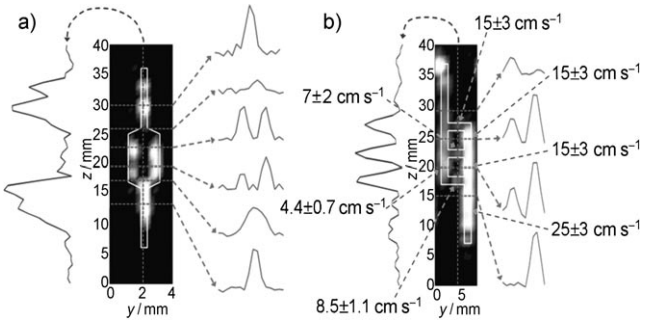

Figure 3. Time projections, one-dimensional profiles, and measured flow velocities: a) Chip 1, b) Chip 2.

indicating that the central part is much thinner than the edge parts. Furthermore, the triangular part between the enlargement and the upper channel is also too thin. A water MRI image (Supporting Information) and optical inspection using dyed water confirmed these conclusions.

The designed channel geometry of Chip 1 is the same as was used in the similar RD experiment carried out with hyperpolarized xenon,[10] and the experimental parameters are comparable. However, the experiment time in the xenon experiment (9 h) was about 50 times longer than that in the propane experiment (10 min) owing to a large number of scans that had to be accumulated because of a much lower sensitivity in the xenon experiment.

Propane gas flow in the ladder-like channel structure of Chip 2 was investigated in the last demonstration (Figure 2d and Supporting Information, Movie 4). The signal amplitudes in the time projection (Figure 3b) imply that the cross-section of the left vertical channel is smaller than that of the right vertical channel. Furthermore, the integrated amplitudes showed that the cross-sections of all the horizontal channels are smaller than those of vertical channels. Water MRI images of the chip (Supporting Information) verified these manufacturing imperfections in the channel geometries. Because of the imperfections, the relative flow velocities measured in different channels (Figure 3b) differ from those predicted by hydrodynamic simulations (Supporting Information).

This work shows that by combining the RD MRI and PHIP techniques, a 10^4–10^5-fold sensitivity enhancement can be achieved, which enables noninvasive, tracerless gas-flow profiling in microfluidic devices. It demonstrates that the TOF images provide versatile information about microfluic flow: They reveal a difference of diffusional mixing in propane gas and water in the capillary tubing and they expose manufacturing imperfections in the channel geometry. The PHIP RD MRI experiments turned out to be one to two orders of magnitude more sensitive than the corresponding RD MRI experiments performed using hyperpolarized xenon, leading to the dramatically shortened experimental times. Furthermore, the developed technique allows scientifically and technologically more fascinating studies to be performed, because parahydrogen can naturally take part in many important chemical reactions, including those performed with the use of microfluidic devices.[23]

Experimental Section

Hyperpolarized propane was obtained in the hydrogenation of propene using parahydrogen catalyzed by supported Wilkinson's catalyst or [Rh(cod)(sulfos)]/SiO_2. Both catalysts provided approximately the same enhancements. The ALTADENA polarization scheme was the most appropriate in this work, because, contrary to the PASADENA scheme,[20] the net signal enhancement appears directly in the NMR spectra without any special spin-system preparation, and a $\pi/2$ RF pulse gives the largest signal amplitude.[24] Consequently, conventional RD MRI encoding procedures can be employed. In RD MRI experiments, outside and inside diameters of the inlet/outlet capillary are 365 and 150 μm, respectively. The encoding coil is a birdcage coil (diameter 25 mm, height 35 mm), and the detection coil (solenoid) inside diameter is 365 μm and length is 3 mm. See Supporting Information for further details.

Received: May 4, 2010
Published online: August 2, 2010

Keywords: heterogeneous catalysis · magnetic resonance imaging · microfluidics · NMR spectroscopy · parahydrogen-induced polarization

[1] G. M. Whitesides, *Nature* **2006**, *442*, 368 – 373.
[2] N.-T. Nguyen, S. T. Wereley, *Fundamentals and Applications of Microfluidics*, Artech House, Boston, **2002**.
[3] K. B. Mogensen, H. Klank, J. P. Kutter, *Electrophoresis* **2004**, *25*, 3498 – 3512.
[4] P. T. Callaghan, *Principles of Nuclear Magnetic Resonance Microscopy*, Clarendon, Oxford, **1991**.
[5] E. Harel, *Lab Chip* **2009**, *9*, 17 – 23.
[6] A. Moule, M. Spence, S.-I. Han, J. Seeley, K. Pierce, S. Saxena, A. Pines, *Proc. Natl. Acad. Sci. USA* **2003**, *100*, 9122 – 9127.
[7] J. A. Seeley, S. I. Han, A. Pines, *J. Magn. Reson.* **2004**, *167*, 282 – 290.
[8] J. Granwehr, E. Harel, S. Han, S. Garcia, P. N. Sen, Y. Song, A. Pines, *Phys. Rev. Lett.* **2005**, *95*, 075503.
[9] E. E. McDonnell, S. Han, C. Hilty, K. L. Pierce, A. Pines, *Anal. Chem.* **2005**, *77*, 8109 – 8114.
[10] C. Hilty, E. E. McDonnell, J. Granwehr, K. L. Pierce, S. Han, A. Pines, *Proc. Natl. Acad. Sci. USA* **2005**, *102*, 14960 – 14963.
[11] I. V. Koptyug, K. V. Kovtunov, S. R. Burt, M. S. Anwar, C. Hilty, S.-I. Han, A. Pines, R. Z. Sagdeev, *J. Am. Chem. Soc.* **2007**, *129*, 5580 – 5586.
[12] L.-S. Bouchard, K. V. Kovtunov, S. R. Burt, M. S. Anwar, I. V. Koptyug, R. Z. Sagdeev, A. Pines, *Angew. Chem.* **2007**, *119*, 4142 – 4146; *Angew. Chem. Int. Ed.* **2007**, *46*, 4064 – 4068.
[13] L.-S. Bouchard, S. R. Burt, M. S. Anwar, K. V. Kovtunov, I. V. Koptyug, A. Pines, *Science* **2008**, *319*, 442 – 445.
[14] K. V. Kovtunov, I. E. Beck, V. I. Bukhtiyarov, I. V. Koptyug, *Angew. Chem.* **2008**, *120*, 1514 – 1517; *Angew. Chem. Int. Ed.* **2008**, *47*, 1492 – 1495.
[15] D. I. Hoult, R. E. Richards, *J. Magn. Reson.* **1976**, *24*, 71 – 85.
[16] V.-V. Telkki, C. Hilty, S. Garcia, E. Harel, A. Pines, *J. Phys. Chem. B* **2007**, *111*, 13929 – 13936.
[17] V.-V. Telkki, J. Saunavaara, J. Jokisaari, *J. Magn. Reson.* **2010**, *202*, 78 – 84.
[18] X. Zhou, D. Graziani, A. Pines, *Proc. Natl. Acad. Sci. USA* **2009**, *106*, 16903 – 16906.
[19] J. Natterer, J. Bargon, *Prog. Nucl. Magn. Reson. Spectrosc.* **1997**, *31*, 293 – 315.
[20] C. R. Bowers, D. P. Weitekamp, *Phys. Rev. Lett.* **1986**, *57*, 2645 – 2648.
[21] P. Bhattacharya, K. Harris, A. P. Lin, M. Mansson, V. A. Norton, W. H. Perman, D. P. Weitekamp, B. D. Ross, *Magn. Reson. Mater. Phys. Biol. Med.* **2005**, *18*, 245 – 256.
[22] M. G. Pravica, D. P. Weitekamp, *Chem. Phys. Lett.* **1988**, *145*, 255 – 258.
[23] R. S. Besser, X. Ouyang, H. Surangalikar, *Chem. Eng. Sci.* **2003**, *58*, 19 – 26.
[24] S. R. Bowers in *Encyclopedia of Nuclear Magnetic Resonance*, *Vol. 9* (Eds.: D. M. Gant, R. K. Harris), Wiley, New York, **2002**, pp. 750 – 769.

